

Tuning colloidal interactions in subcritical solvents by solvophobicity: Explicit versus implicit modeling

J. Dzubiella,^{1,a)} J. Chakrabarti,^{2,b)} and H. Löwen^{3,c)}

¹*Department of Physics, Technical University Munich, 85748 Garching, Germany*

²*Statistical and Soft Condensed Matter Physics, S N Bose National Centre for Basic Sciences, Kolkata 700 098, India*

³*Institut für Theoretische Physik, Heinrich-Heine Universität, Universitätsstrasse 1, 40225 Düsseldorf, Germany*

(Received 2 June 2009; accepted 9 July 2009; published online 28 July 2009)

The distance-resolved effective interaction between two colloidal particles in a subcritical solvent is explored both by an explicit and implicit modeling. An implicit solvent approach based on a simple thermodynamic interface model is tested against grand-canonical Monte Carlo computer simulations using explicit Lennard-Jones solvent molecules. Close to liquid-gas coexistence, a joint gas bubble surrounding the colloidal particle pair yields an effective attraction between the colloidal particles, the strength of which can be vastly tuned by the solvophobicity of the colloids. The implicit model is in good agreement with our explicit computer simulations, thus enabling an efficient modeling and evaluation of colloidal interactions and self-assembly in subcritical solvent environments.

© 2009 American Institute of Physics. [DOI: [10.1063/1.3193557](https://doi.org/10.1063/1.3193557)]

I. INTRODUCTION

In solution, a colloidal or nanosized particle with a solvophobic surface has a strong tendency to form voids or cavities around it in order to avoid the high particle-solvent interfacial free energy. In particular, in a subcritical solvent close to its bulk liquid-gas transition, a gas bubble can be formed around the solvophobic solute the size of which is governed by the degree of solvophobicity and the distance to the gas-liquid transition.¹⁻³ The collective behavior of many solute particles will be strongly affected by the presence of covering gas bubbles which can trigger capillary cavitation between the particles. In fact, the resulting strong effective attractions will push neighboring particle together resulting in a single joint gas bubble which contains more than a single particle.^{1,4-6} Recently, this effect has been exploited to create new morphological structures composed of colloidal superparticles.⁷ There are also ideas to use solvophobic nanoparticle to control drying-mediated hierarchical self-assembly.⁸ Last but not least, proteins with extended hydrophobic surfaces can be surrounded by a cavity depleted from water which can also lead to capillary evaporation and a strong hydrophobic collapse.^{9,10} The formation of a (water) vapor bubble in proteins may be the rate-limiting step in the folding of certain types of proteins.¹¹ Therefore a general molecular understanding of the effective interactions between solvophobic particles is desirable. In detail, clear predictions about how to tune the effective interactions by changing solvophobicity and the thermodynamic parameters of the solvent will be helpful to control and steer material properties.

There have been a number of computer simulation studies for solvophobic solutes in which the solvent is treated explicitly, for example by hard spheres,¹² Lennard-Jones (LJ) particles,^{6,13-16} or other models more appropriate for organic solvents¹⁷ and water.^{18,19} Density functional theory^{20,21} and liquid integral equation studies²²⁻²⁴ which include the solvent interparticle interactions have also been employed for the effective interactions between two bubbled nanoparticles.²⁴ On the other hand, more coarse-grained thermodynamic approaches which work in terms of surface (or line) tensions have been proposed.^{1,25-28} In these approaches, the discrete nature of the solvent is neglected, i.e., it is an implicit modeling where the solvent is treated as a continuum.

The aim of this paper is to compare the explicit and implicit modeling for the effective interactions between two solvophobic colloidal particles in a subcritical solvent in dependence of their degree of solvophobicity. In order to do so we employ a minimalistic two-dimensional (2D) model of a discrete LJ solvent which was studied earlier in detail¹⁵ and captures the essential physics. Furthermore, an implicit model proposed previously^{27,28} is getting topologically easier in two dimensions. In fact with an appropriate choice of the phenomenological input parameters needed for the implicit solvent models, we find good agreement between the implicit and explicit modeling for various degrees of solvophobicity. Both the distance-resolved effective attraction and the location of the bubble interface are described well in the implicit solvent approach. The dependence of the attraction strength on the solvophobicity also coincides in the two approaches. For future studies and applications, our findings facilitate a quick estimate about the trends and rough parameters for various systems within the implicit approach.

The paper is organized as follows: in Sec. II, the system is described and both methods (explicit and implicit)

^{a)}Electronic mail: jdzubiel@ph.tum.de.

^{b)}Electronic mail: jaydeb@bose.res.in.

^{c)}Electronic mail: hloewen@thphy.uni-duesseldorf.de.

are briefly outlined. Results are presented and discussed in Sec. III revealing good agreement between the implicit and explicit approach. Finally we conclude in Sec. IV.

II. SYSTEM AND METHODS

A. Two colloids in a subcritical liquid

We consider a model system in 2D space in which two colloids (solutes) are immersed in a subcritical solvent modeled by isotropic LJ interactions. The interaction between two solvent particles at separation r is thus given by the LJ pair potential, $V_{\text{LJ}}(r) = 4\epsilon[(\sigma/r)^{12} - (\sigma/r)^6]$, where σ defines the length scale in the system. The interaction parameter ϵ is taken at a subcritical temperature ($k_B T / \epsilon = 0.45$), where $k_B T$ is the thermal energy. The chemical potential is held fix at $\mu / k_B T = -3.7$ which is found to be $\approx 0.1 k_B T$ below that of the gas-liquid coexistence for the chosen parameters,¹⁵ and the stable bulk phase of the solvent particles being liquid. The bulk liquid and gas number densities at this state point have been calculated to be $\rho_0 = 0.72 \sigma^{-2}$ and $0.04 \sigma^{-2}$, respectively.¹⁵

We consider the infinite dilution limit of the colloids and therefore focus on the pair interaction between two colloids which are placed at a fixed mutual distance s . The interaction between a colloid at $\vec{R}_i = (X_i, Y_i)$ with $i = 1, 2$ and a solvent particle at $\vec{r} = (x, y)$ is given by a modified LJ form

$$V_{cs}(r_i) = 4\epsilon_{cs} \left[\left(\frac{\sigma}{r_i - R_0} \right)^{12} - \lambda \left(\frac{\sigma}{r_i - R_0} \right)^6 \right], \quad (1)$$

where $r_i = |\vec{R}_i - \vec{r}|$, $R_0 = 2.5\sigma$ is the hard-core radius of the colloids, and the dimensionless ‘‘solvophobicity parameter’’ λ tunes the dispersion attraction between the colloids and the solvent particles. Note that $\lambda = 0$ corresponds to a purely repulsive solvophobic interaction between the colloids and the solvent for which isolated colloids are observed to be covered by a thin layer of gas.¹⁵ Similarly, $\lambda = 1$ corresponds to the pure LJ potential, namely, a dominantly solvophilic interaction. Thus one can interpolate from the solvophobic to solvophilic interactions by gradually increasing λ . We further fix $\epsilon_{cs} / \epsilon = 5.0$. As we are just interested in the solvent-mediated interaction the mutual colloidal interaction is simply modeled as hard core like with a hard-core diameter of $2R_0$.

B. Grand canonical Monte Carlo simulations

The particles are taken in a cubic simulation box of size 50σ with periodic boundary conditions in all the directions. The solvent particle positions are updated using the grand-canonical Monte Carlo (GCMC) method.²⁹ Typically for a given λ , first 10^5 runs have been discarded for the equilibration, after which the production run has been 5×10^5 steps long. The data have been collected every five steps during the production run. The long averaging has been essential to capture the interfacial distribution of the solvent particles between two solute particles due to typically low density of the solvent particles. More details of the simulations are given elsewhere.¹⁵

After equilibration we calculate the density distribution $\rho(\vec{r})$ of the solvent around the colloids and the effective solvent-mediated force between the two colloids at positions \vec{R}_1 and \vec{R}_2 defined by $F_{\text{eff}}(s) = \langle -[\nabla_1 \Sigma_i V_{cs}(|\vec{r}_i - \vec{R}_1|)] \cdot \vec{R}_{12} \rangle$, where $\vec{R}_{12} = \vec{R}_1 - \vec{R}_2$, $s = |\vec{R}_{12}|$, and the gradient operator is over the coordinate of the first solute. In order to estimate the interface location between the solvent and the solutes from the simulations we take the density profiles $\rho(\vec{r})$ and define the interface line to be at the equidensity loci, where $\rho(\vec{r}_{\text{int}}) = \rho_0 / 2.0$. Given the loci $\{\vec{r}_{\text{int}}\}$, the interface shape in our 2D system can thus be conveniently expressed by a one-dimensional (1D) function $y(x)$, where x is the coordinate along the symmetry axis along the connection line $y = 0$ between the colloid centers.

C. Implicit solvent model

We compare our simulation results to an implicit solvent model or *interface model* in which the description of the solvent degrees of freedom is reduced to a continuous (solute-solvent) interface and three macroscopic parameters, namely, the pressure P , the line tension γ , and the solvent density ρ_0 . In our 2D system under consideration the interface is a 1D curve in space. The interface model is based on a variational formalism in which the solvation free energy is defined as a functional of the interface geometry and then minimized to give the shape equation for evaluation of the interface. For this, let us define a subregion \mathcal{A} empty of solvent in total 2D space Ω for which we assign an area exclusion function $a(\vec{r}) = 0$ for $\vec{r} \in \mathcal{A}$ and $a(\vec{r}) = 1$ else, and $\vec{r} = (x, y)$ is a 2D vector. The absolute area A and interface length L of \mathcal{A} can then be expressed as functionals of $a(\vec{r})$ via $A[a] = \int_{\Omega} d^2r [1 - a(\vec{r})]$ and $L[a] = \int_{\Omega} d^2r |\nabla a(\vec{r})| = \int_{\partial\Omega} dL$. Thus, A and L define the solvent-accessible area and surface line, respectively, and the solvent density is $\rho(\vec{r}) = \rho_0 a(\vec{r})$, where ρ_0 is the bulk value. The solvation free energy G is proposed to be a *functional* of the geometry $a(\vec{r})$ of the form

$$G[a] = PA[a] + \gamma \int_{\partial\Omega} dL + \rho_0 \int_{\Omega} d^2r a(\vec{r}) U(\vec{r}), \quad (2)$$

where γ is the liquid-vapor line tension, and $U(\vec{r}) = \sum_{i=1}^2 V_{cs}(\vec{r} - \vec{R}_i)$ adds up the LJ interactions between the solutes at \vec{R}_1 and \vec{R}_2 and the solvent at position \vec{r} in a mean-field way. The last term on the right hand side of Eq. (2) thus describes the solvophobic or solvophilic interaction energy of the solutes with the solvent depending on the interface location and is tuned by the parameter λ introduced before in Eq. (1). Applying the calculus of differential geometry and functional derivatives, the minimization $\delta G[a] / \delta a(\vec{r}) = 0$ leads to the ordinary differential equation (ODE)

$$0 = P - \gamma \kappa(\vec{r}) - \rho_0 U(\vec{r}) =: \text{ODE}(\vec{r}), \quad (3)$$

which is a 2D Laplace equation of classical capillarity³⁰ but extended by the term coupled to the solvent density to capture the influence of local solute-solvent dispersion interactions. The quantity $\kappa(\vec{r})$ in the second order ODE (3) is the local curvature. The ODE has no analytical solution in our case and has to be solved numerically. Once the interface

line is determined, its shape can be plugged back into the energy functional (2) to obtain the solvation free energy of the two solutes. Doing so for different colloidal distances s we obtain, within an arbitrary energy constant G_0 , the effective interaction energy $v_{\text{eff}}(\vec{s}) = G([a]; \vec{s})$ between the two colloids. The force is then $\vec{F}_{\text{eff}}(s) = -\nabla v_{\text{eff}}(s)$. A similar interface model based on the same variational formalism was introduced in detail previously for water in three-dimensional space including curvature corrections and electrostatic interactions^{27,28} and has been applied to the solvation of non-polar molecular solutes.³¹

1. Shape function and numerical evaluation

For the numerical solution of the interface model the curvature can be conveniently parametrized by functions $y(l)$ and $x(l)$ which describe the 1D interface curve in space with the arc length l as the parameter. The curvature κ is then given by

$$\kappa(x, y) = \frac{x'y'' - y'x''}{(x'^2 + y'^2)^{3/2}}, \quad (4)$$

where the primes indicate the partial derivative with respect to l . Additionally, the unit normal vector to the interface reads

$$\vec{n}(x, y) = \frac{1}{\sqrt{x'^2 + y'^2}} \begin{pmatrix} x' \\ -y' \end{pmatrix}. \quad (5)$$

The ODE (3) is then solved by a forward relaxation scheme using the “time” parameter t ,

$$\begin{pmatrix} x(t + \Delta t) \\ y(t + \Delta t) \end{pmatrix} = \begin{pmatrix} x(t) \\ z(t) \end{pmatrix} - \Delta t \vec{n}(x, y) \text{ODE}(x, y), \quad (6)$$

where the steady-state solution $\partial(x, y)/\partial t = 0$ is the solution of $\text{ODE}(x, y) = 0$ we are looking for. Both colloids are held at a fixed distance s in the numerics as in the simulation. In the numerical calculations we use a grid of 500 bins and an integration time step of $\Delta t = 0.001$. The first and second derivatives are approximated using a symmetric two- and three-step finite difference equation, respectively. Convergence is usually reached after 10^5 time steps. The result can be expressed by a *shape function* $y(x)$ which describes the solute-solvent interface line. The interface shape is observed to be dependent of the initial form of the shape line $y(x)$ at $t=0$, which is either chosen to loosely envelope both colloids or it envelopes either one of them individually. The former initial boundary line typically leads to the “dry branch” of the solution (where a gas bubble is found between the solutes) while the second initial boundary line leads to the “wet branch” (i.e., no bubble), as observed in previous studies on dewetting.³² Both solutions are topologically different as they correspond to either one single area void of solvent or two separated areas void of solvent, respectively.

III. RESULTS AND DISCUSSION

A. Repulsive-only solute-solvent interactions ($\lambda=0$)

In the first step we compare the interface model to the GCMC simulations for the repulsive-only solute-solvent in-

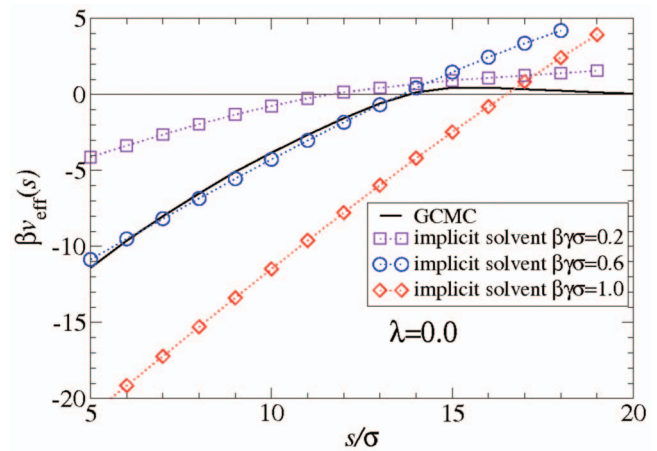


FIG. 1. Effective interaction $v_{\text{eff}}(s)$ between the two colloids vs their mutual distance s for the repulsive-only solute-solvent interaction case ($\lambda=0$). The implicit solvation results (circles) are compared to the GCMC simulations (solid line) for line tension parameters $\beta\gamma\sigma = \gamma/(k_B T/\sigma) = 0.2, 0.6$, and 1.0 .

teraction case ($\lambda=0$) which will allow us to extract the line tension parameter γ for the system under consideration. The second input parameter, the density ρ_0 is determined directly by the computer simulations¹⁵ to be $\rho_0 = 0.72\sigma^{-2}$ and remains fixed throughout the following. For the third input parameter, the pressure P , an upper estimate is possible by using the fact that our system is subcritical and thermodynamically close to coexistence. In this case the pressure can be expanded and estimated by $P \approx \Delta\mu\Delta\rho$, where $\Delta\mu = \mu - \mu_{\text{crit}}$ is the deviation from the chemical potential to the critical value and $\Delta\rho = \rho_l - \rho_g$ is the gas-liquid density difference. From the analysis of the GCMC system¹⁵ we obtain $\Delta\mu \approx 0.1k_B T$ and $\Delta\rho = 0.68\sigma^{-2}$, and thus get an upper estimate of about $P \approx 0.1k_B T \cdot 0.68\sigma^{-2} \approx 0.07k_B T\sigma^{-2}$ which we will use in the following.

In order to estimate the line tension parameter γ we solve ODE (3) for the repulsive-only solute-solvent interaction case ($\lambda=0$) and compare the results to the available GCMC simulation data for the mutual colloidal interaction $v_{\text{eff}}(s)$.¹⁵ To estimate the arbitrary energy constant G_0 we define the reference state (where $v_{\text{eff}}=0$) to be the wet state of the colloids at infinite distance, i.e., G_0 is given by the value of the wet energy branch at $s \rightarrow \infty$ and is found to be $G_0 \approx 34.5k_B T$. For the comparison to the GCMC results we subtract G_0 from the dry energy branch. The GCMC data are replotted in Fig. 1 together with the numerical solution for the dry branch of ODE (3) for $\lambda=0$ and three different values of $\gamma = 0.2, 0.6$ and $1.0k_B T/\sigma$ (symbols). First of all we observe that the interface model result is in qualitative agreement with the GCMC data: Both results feature a strong, monotonic attraction which almost linearly decays from the contact distance $s \approx 5\sigma$ up to $s \sim 15\sigma$. The slope of the interaction energy from the interface model is dominated by the value of the line tension γ . A best fit to the GCMC interaction slopes in Fig. 1 yields a line tension value of $\gamma \approx 0.6k_B T/\sigma$, which we use in Sec. III B to *predict* the action of increasing solvophobicity ($\lambda > 0$) on the colloidal interaction with our interface model.

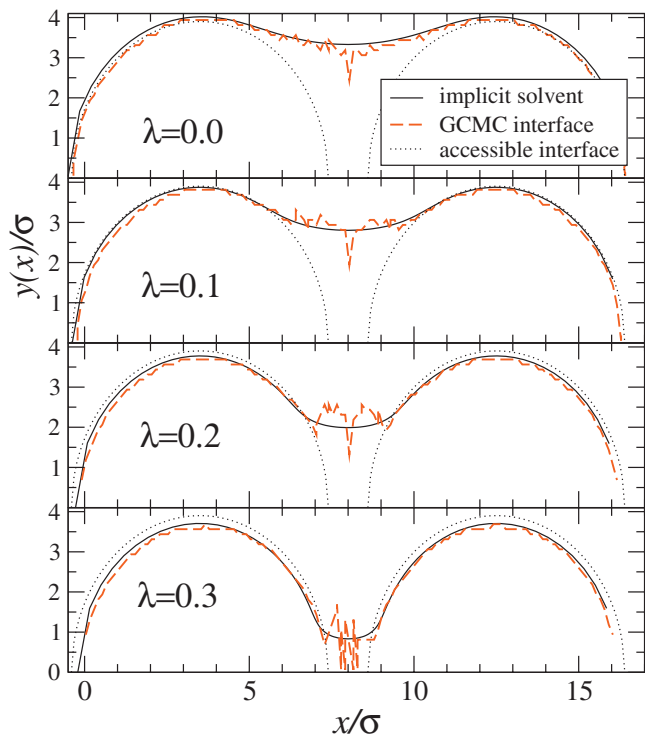


FIG. 2. Solute-solvent interface shape function $y(x)$ for the two colloids (solutes) placed at a fixed distance $s=9\sigma$ for different values of the solute-solvent attraction parameter $\lambda=0.0, 0.1, 0.2,$ and 0.3 . The interface model results (solid lines) are in good agreement with the GCMC simulation results (dashed lines) within their statistical error. The dotted lines show the contour of the spheres at a radius $R=3.9\sigma$ which is the solvent-accessible sphere radius at a distance $s=\infty$.

By inspecting the interface shape $y(x)$ in the attractive region we find that the strong attraction is accompanied by the formation of a *vapor bubble* in between the (solvophobic) colloids. An example is plotted in Fig. 2 for $s=9\sigma$ (and $\lambda=0.0$) where the simulation and interface model are directly compared and show excellent conformity. This supports the validity of the simple interface model and explains that the strong attraction in the system is dominated by the urge of the system to minimize unfavorable interface length; this pushes the colloids together until they touch. At the critical distance $s^*\approx 14\sigma$, where the attraction vanishes, cf. Fig. 1, the bubble is observed to rupture in the GCMC simulation leading to completely wet colloids. In quantitative agreement, the interface model also shows a vanishing attraction at s^* . Note, however, that the dry branch of ODE (3) converges to energies larger than 0 for distances greater than the critical distance $s^*\approx 14\sigma$ leading to positive energy values for $s>s^*$ in Fig. 1, as observed previously in dewetting geometries.³² This can be attributed to the metastability of the dry energy branch at large distances $s>s^*$ due to a (nucleation) energy barrier between vapor and wet states as known for subcritical LJ solvents and water in solvophobic confinement.^{33–35} The numerical evolution of ODE (3) we perform is apparently not able to overcome this energy barrier.

B. Influence of solvophobicity

To study the influence of enhanced solvophilicity (diminished solvophobicity) we fix the distance between the

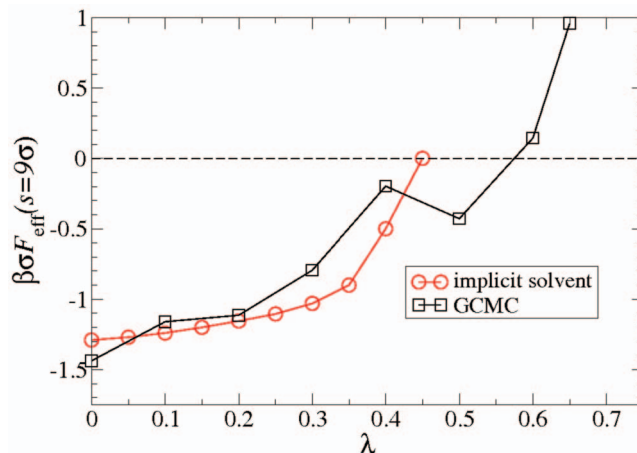


FIG. 3. Effective interaction force $F_{\text{eff}}(s)$ between the two colloids (solutes) placed at a distance $s=9\sigma$ vs the solvophobicity parameter λ . The strong attraction for $\lambda=0$ decreases for increasing λ and vanishes at a critical value of $\lambda\approx 0.4$. The prediction of the interface model (circles) is in good agreement with the GCMC simulation results (squares).

colloids at $s=9\sigma$ for the sake of clarity (without loss of generality) and increase the attraction parameter λ in interaction (1). Physically that means that the colloids attract the solvent more and more, and the observed vapor bubble between the colloids is expected to shrink. Inspecting Fig. 2, where we plot the interface shape $y(x)$ for $\lambda=0.1, 0.2,$ and 0.3 , this is exactly what is happening. Clearly visible, the interface part in the symmetry center [$y(x\approx 8\sigma)$] decreases significantly from $\approx 3.2\sigma$ for $\lambda=0$ to $\approx 0.8\sigma$ for $\lambda=0.3$. The prediction of the interface model and the GCMC simulations are still in good agreement within the simulation statistics. Note also that the interface further away from the bubble [$y(x\leq 3)$ or $y(x\geq 13)$] wraps the colloids tighter with increasing λ in both explicit and implicit approaches. Increasing the solute-solvent attraction further leads to a complete wetting of the colloids for $\lambda\geq 0.4$ in both GCMC and interface model (not shown). Interestingly, as opposed to the $\lambda=0$ case for larger distances $s>s^*$, the numerical evaluation captures the transition from the dry to wet state, perhaps due to a vanishing energy barrier along the physical (or numerical) pathway.

The change in solute-solvent interaction and concomitant interface shape has a strong influence on the colloid-colloid interaction. This is demonstrated for the effective interaction force $F_{\text{eff}}(s)$ in Fig. 3 for a fixed solute distance $s=9\sigma$ and increasing λ values. The strong attraction of $F_{\text{eff}}(s=9\sigma)\approx -1.4k_B T/\sigma$ observed for $\lambda=0$ decreases for increasing λ and vanishes at a critical value of $\lambda\approx 0.4$, which corresponds well to the complete wetting of the solutes by solvent [$y(x\approx 8\sigma)=0$]. The prediction of the interface model is in quantitative agreement with the GCMC simulation results within the statistical error. Physically, the colloids prefer to be wet (as they are attracted to the solvent) for $\lambda\geq 0.4$ and want to stay in solution. Their mutual attraction vanishes as correctly explained by the interface model. In the GCMC simulation even repulsion between the colloids is visible for $\lambda\geq 0.6$. This can be attributed to crowding of solvent particles between the two colloids pushing them apart.^{6,15} This correlation effect due to the coarse structure of

the solvent cannot be captured by the interface model which is based on simple interface thermodynamics and mean-field energetics.

IV. CONCLUSION

In conclusion, an implicit solvent approach has been tested against explicit solvent computer simulations for the interaction between two solvophobic colloids in a subcritical solvent and good agreement was found. The strong effective attraction found between the colloids, but which is very sensitive to their degree of solvophobicity, can be attributed to bubble formation around the solvophobic particles. This exemplifies the interesting and important new physics induced by the nearby location in phase space of a drying transition. The effective solute-solvent interface locations from the GCMC calculation can be accurately predicted by the implicit model and an intimate connection between interface shape, local solute-solvent dispersion interactions, and the mutual colloid interaction is found. Our findings enables one to employ the computationally much more efficient implicit solvent model for situations where a direct explicit computer simulation is not straightforward, e.g., for polarizable molecular solvents, highly polydisperse, or size-asymmetric systems, or for solutes with many degrees of freedom or complex geometries such as proteins,³⁶ where strong collective effects become important.

Future studies should address the three-dimensional case. Also the inclusion of a curvature correction to the surface tension may be important for sufficiently high interface curvature but may be nonanalytic in curvature below a certain length scale due to the drying effect.²¹ Another issue concerns the inclusion of electrostatic interactions between solute and solvent which may be possible on a mean-field (Poisson-Boltzmann) level.²⁸ Moreover, the “inverse” thermodynamic situation of a bridging *wetting layer* around a *solvophilic* solute¹ can similarly be treated by explicit and implicit modeling and we expect a similar performance of the implicit model here. It would be additionally challenging to generalize the implicit model to nonequilibrium situations where the solute particles are sheared and dragged away by external fields.^{16,37,38}

ACKNOWLEDGEMENTS

J.D. is grateful to the Deutsche Forschungsgemeinschaft (DFG) for support within the Emmy-Noether-Program. This work was also supported by the DFG within the SFB TR6 (project section D3).

- ¹P. A. Kralchevsky and N. D. Denkov, *Curr. Opin. Colloid Interface Sci.* **6**, 383 (2001).
- ²J. R. Henderson, *J. Chem. Phys.* **116**, 5039 (2002).
- ³M. C. Stewart and R. Evans, *Phys. Rev. E* **71**, 011602 (2005).
- ⁴R. F. Considine and C. J. Drummond, *Langmuir* **16**, 631 (2000).
- ⁵M. A. Hampton and A. V. Nguyen, *J. Colloid Interface Sci.* **333**, 800 (2009).
- ⁶H. Shinto, M. Miyahara, and K. Higashitan, *J. Colloid Interface Sci.* **209**, 79 (1999).
- ⁷J. Q. Zhuang, H. M. Wu, Y. G. Yang, and Y. C. Cao, *Angew. Chem.* **47**, 2208 (2008).
- ⁸O. Kletenik-Edelman, E. Ploshnik, A. Salant, R. Shenhar, U. Banin, and E. Rabani, *J. Phys. Chem. C* **112**, 4498 (2008).
- ⁹D. Chandler, *Nature (London)* **437**, 640 (2005).
- ¹⁰B. Berne, J. Weeks, and R. Zhou, *Ann. Rev. Phys. Chem.* **60**, 85 (2009).
- ¹¹P. R. ten Wolde and D. Chandler, *Proc. Natl. Acad. Sci. U.S.A.* **99**, 6539 (2002).
- ¹²E. Allahyarov and H. Löwen, *J. Phys.: Condens. Matter* **13**, L277 (2001); *Phys. Rev. E* **63**, 041403 (2001).
- ¹³Y. Qin and K. A. Fichthorn, *J. Chem. Phys.* **119**, 9745 (2003).
- ¹⁴H. Greberg and G. N. Patey, *J. Chem. Phys.* **114**, 7182 (2001).
- ¹⁵J. Chakrabarti, S. Chakrabarti, and H. Löwen, *J. Phys.: Condens. Matter* **18**, L81 (2006).
- ¹⁶J. Chakrabarti and H. Löwen, *J. Chem. Phys.* **129**, 134507 (2008).
- ¹⁷Y. Qin and K. A. Fichthorn, *Phys. Rev. E* **74**, 020401 (2006).
- ¹⁸J. Dzubiella and J. P. Hansen, *J. Chem. Phys.* **119**, 12049 (2003).
- ¹⁹J. Dzubiella and J. P. Hansen, *J. Chem. Phys.* **121**, 5514 (2004).
- ²⁰C. Bauer, T. Bieker, and S. Dietrich, *Phys. Rev. E* **62**, 5324 (2000).
- ²¹R. Evans, J. R. Henderson, and R. Roth, *J. Chem. Phys.* **121**, 12074 (2004).
- ²²E. Rabani and S. A. Egorov, *Nano Lett.* **2**, 69 (2002).
- ²³E. Rabani and S. A. Egorov, *J. Phys. Chem. B* **106**, 6771 (2002).
- ²⁴S. D. Overduin and G. N. Patey, *J. Chem. Phys.* **123**, 194505 (2005).
- ²⁵H. Löwen, *Phys. Rev. Lett.* **74**, 1028 (1995); *Z. Phys. B* **97**, 269 (1995).
- ²⁶P.-M. König, R. Roth, and K. R. Mecke, *Phys. Rev. Lett.* **93**, 160601 (2004).
- ²⁷J. Dzubiella, J. Swanson, and J. A. McCammon, *Phys. Rev. Lett.* **96**, 087802 (2006).
- ²⁸J. Dzubiella, J. Swanson, and J. A. McCammon, *J. Chem. Phys.* **124**, 084905 (2006).
- ²⁹M. P. Allen and D. J. Tildesley, *Computer Simulation of Liquids* (Clarendon, Oxford, 1987).
- ³⁰P.-G. de Gennes and F. Brochart-Wyart, *Capillary and Wetting Phenomena* (Springer, New York, 1983).
- ³¹L.-T. Cheng, J. Dzubiella, J. A. McCammon, and B. Li, *J. Chem. Phys.* **127**, 084503 (2007).
- ³²K. Lum, D. Chandler, and J. Weeks, *J. Phys. Chem. B* **103**, 4570 (1999).
- ³³A. Vishnyakov and A. V. Neimark, *J. Chem. Phys.* **119**, 9755 (2003).
- ³⁴K. Leung and A. Luzar, *J. Chem. Phys.* **113**, 5845 (2000).
- ³⁵K. Leung, A. Luzar, and D. Bratko, *Phys. Rev. Lett.* **90**, 65502 (2003).
- ³⁶H. Hansen-Goos, R. Roth, K. R. Mecke, and S. Dietrich, *Phys. Rev. Lett.* **99**, 128101 (2007).
- ³⁷H. Löwen, *J. Phys.: Condens. Matter* **13**, R415 (2001).
- ³⁸J. Dzubiella, H. Löwen, and C. N. Likos, *Phys. Rev. Lett.* **91**, 248301 (2003).